On-Chip Tunable Mode-Locked Comb Laser in Generic Foundry Platform

Mu-Chieh Lo,* Alex Bennett, Zichuan Zhou, Alfonso Ruocco, Zhixin Liu
Optical Networks Group, University College London (UCL), London, United Kingdom
**m.lo@ucl.ac.uk*

Abstract:
An integrated, passive, harmonically mode-locked laser fabricated utilizing a generic integration technology is reported. The device features both emission wavelength and comb spacing variability by using a colliding-pulse cavity composed of two tunable gratings.

1. Introduction

Chip-scale optical frequency combs have been widely employed for optical communication applications, including wavelength division multiplexed network [1], microwave and terahertz transmission [2], and clock synchronization and distribution [3]. Among the comb generation methods, passive mode locking (PML) requires neither any additional optical (as pump or seed) nor RF modulation signal, making it relatively simple and compact [4]. However, emission wavelength and mode spacing of a PML comb are determined by the device composition and structure; hence usually hard to vary unless a tunable element is in place. Spectral selectivity of PML has been achieved using an as-cleaved distributed Bragg reflector (DBR) [5]. However, limitations in cleaving precision prevent the reproducibility of such a device.

The introduction of the generic foundry approach has brought design freedom since it allows for the arbitrary placement of performance-verified building blocks on a photonic integrated chip [6]. As a result, the cleaving requirement can be relieved, and a mode-locked laser can be integrated with other components to enable versatile functionalities and spectral flexibility [7]. Harmonic mode-locking, which increases the mode spacing beyond the fundamental frequency of the cavity, has been obtained by incorporating an arrayed waveguide grating (AWG) [8] and a Mach-Zehnder interferometer (MZI) [9]. However, the harmonic orders in these designs are not variable. In Ref. [10], researchers presented that intra-cavity electro-refractive modulators could permit a small spectral tuning range, showing a 1.6 MHz mode spacing tuning range and a 1.01 GHz wavelength variation. In Ref. [11], by tuning an intra-cavity DBR in an anti-colliding design, the spectrum shifted towards shorter wavelengths by 9 nm, however, the mode spacing variation was limited to $\sim$100 MHz.

In this paper, we present a new PML comb generator using a generic foundry technology. This design permits spectral variability of both mode spacing and emission wavelength. Such variability is attributed to the combination of harmonic mode locking and tunable DBR reflectors in the generic integration approach, which is presently unseen in literature. Our design enables DC-controlled switchability of mode spacing in harmonic frequencies of 17.5, 35, and 70 GHz. We also demonstrate a 3 nm emission wavelength running by simply adjusting the DC operation conditions, benefiting applications such as wavelength switching.

2. Device design and fabrication

Our PML device was fabricated with an active-passive layer stack realized by regrowth steps on a single semi-insulating (SI) InP substrate [12], which is accessible through a multi-project wafer (MPW). Fig.1 shows the top view of the proposed design and implemented sample, in a 3.3 mm (width) by 0.6 mm (height) area. As shown in Fig. 1(a), the PML consists of multi-quantum well (MQW) active components including a 50 µm long saturable absorber (SA) and the two 500 µm long semiconductor optical amplifier (SOA). Two 500 µm current-injection phase modulators (CIPM) enclosed by the two 50 µm Bragg reflectors (DBR) were fabricated in a Q(1.3) quaternary bulk waveguide layer. The cavity length of the PML is 2.4 mm, corresponding to a fundamental round-trip rate of roughly 17.5 GHz. The SA is placed in the center, where two counter-propagating pulses collide, enabling (second-order) harmonic mode locking.

Isolation sections were inserted between the active sections to isolate the p-regions, while the n-regions at both sites share the same potential. Active-passive butt joints and transition sections were placed to couple the intra-cavity active waveguides (WG) to the outer passive WGs. The passive WGs lead to the cleaved facets on either side of the chip. Fig. 1(b) shows that the symmetric configuration has an electrical contact pad for each

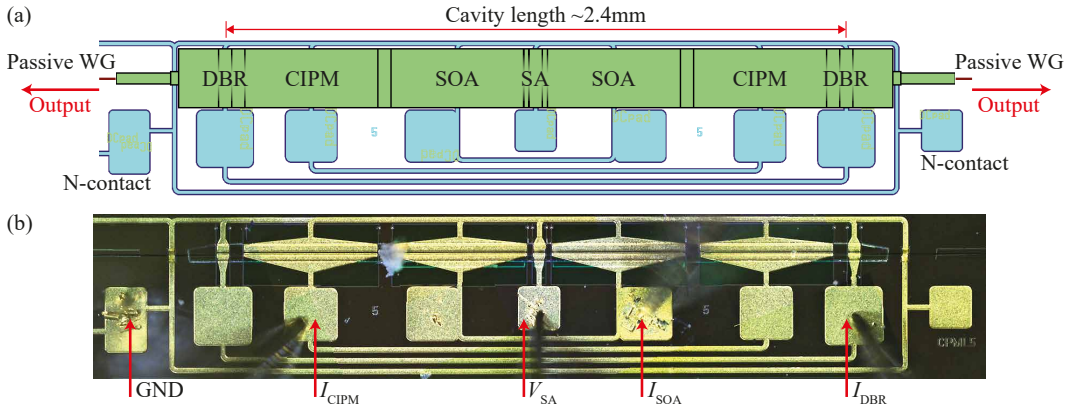

Fig. 1. (a) Layout and (b) photo of the DBR colliding-pulse mode-locked laser.

active section, and interconnects, made in pairs, are also situated symmetrically about the central SA. Using the electrical interconnects, both active elements in each pair share the same electrical signal. In the experimental testing, probes were used to feed electrical currents and voltages to the active components via the contact pads and the interconnects. The SOAs provided the optical gain and were pumped with a current source I_{SOA}. The SA was biased with a voltage source V_{SA}.

3. Device characterization

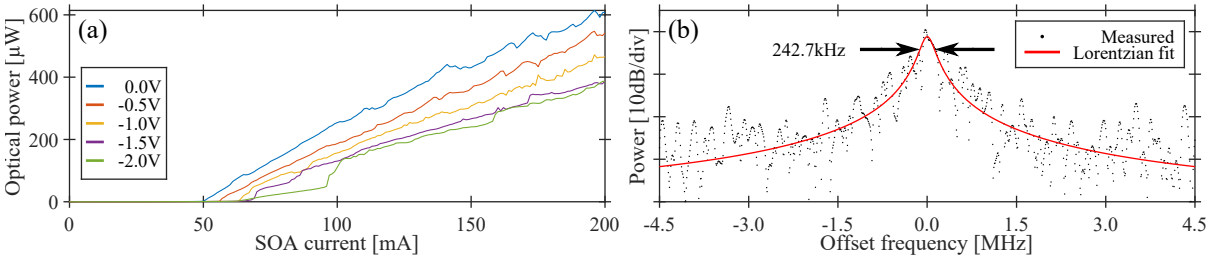

Fig. 2. (a) LI curves: Fiber-coupled power versus laser injection current I_{SOA} for reverse bias voltage V_{SA}. (b) Beatnote at 2nd harmonic frequency. Resolution bandwidth: 100 kHz. Center frequency: 34.865 GHz.

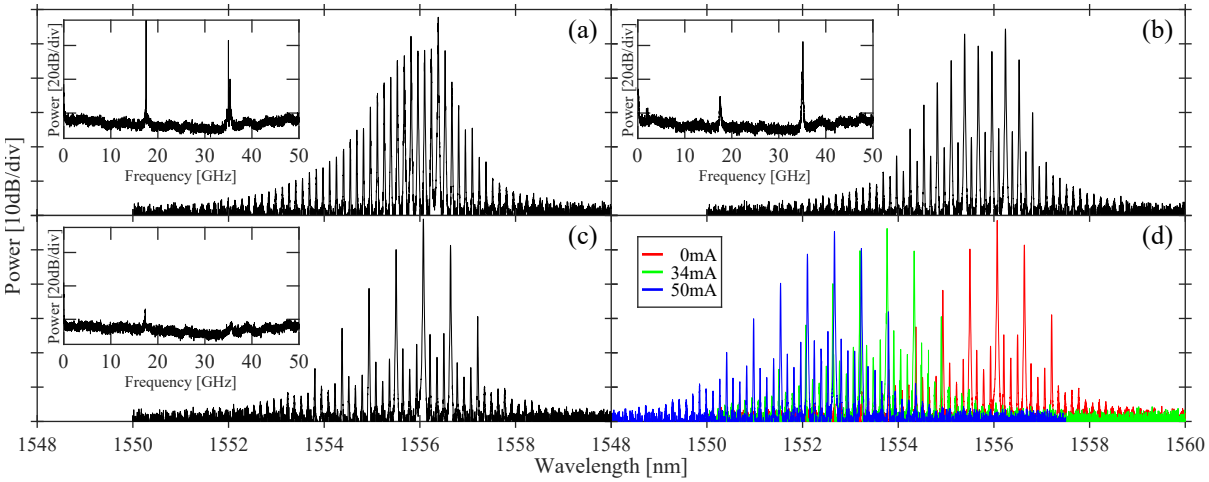

Fig. 3. Optical spectra of the passively mode-locked laser under the conditions of (a) 1st fundamental, (b) 2nd harmonic, (c) 4th harmonic mode locking, and (d) wavelength shifting by various tunable grating injection currents I_{DBR}. Resolution bandwidth: 0.01 nm. Insets show the corresponding electrical spectra.

The chip was stabilized at 25°C. The PML device emitted light through a cleaved facet output waveguide with an anti-reflection coating. It was edge-coupled to a lensed single-mode fiber (mode-field diameter of 3 μm) followed by a dual-stage optical isolator. The output light was split three ways to an optical spectrum anlayzer, an optical

power meter (for light-current LI measurement), and a 40 GHz photodiode connecting to an electrical spectrum analyzer for beat linewidth characterization.

The measured LI characteristics at different reverse bias voltages are depicted in Fig 2(a) after the optical splitting ratio losses have been calibrated. Note that the measurements were taken in the presence of ∼6 dB chip-to-fiber coupling loss. The various reverse bias voltages (from 0 to -2 V) applied onto the SA are labeled on the respective LI curves. The maximum DC SOA current was limited to 200 mA to avoid deleterious heating of the device. For V_{SA} = 0 V, the threshold current is 48 mA. With a higher reverse-bias voltage applied to the SA, the intra-cavity absorption increases leading to a higher threshold current and lower slope efficiency. Fig. 2(b) shows the measured beatnote spectrum at a center frequency of 34.865GHz using I_{SOA} = 175.0 mA and V_{SA} = -0.90 V. The second-order beatnote peak frequency is ∼34.865 GHz, twice the cavity round-trip frequency for this condition. The 3-dB RF linewidth is estimated to be 242.7 kHz, obtained from a Lorentzian fit confirming that mode locking has occurred at the second harmonic frequency, which agrees with the design.

The optical spectra for selected operation conditions are shown in Fig. 3, with a resolution bandwidth of 0.01 nm. For I_{SOA} = 180.0 mA, V_{SA} = 0 V, the PML spectrum is depicted in Fig. 3(a) with emission wavelengths around 1556 nm and a ∼ 0.8-nm 3-dB bandwidth. The 0.14 nm mode spacing corresponds to a repetition rate of 17.5 GHz, confirmed by the photodetected RF spectrum (see inset). For I_{SOA} = 175.0 mA, V_{SA} = -0.90 V, the PML spectrum is depicted in Fig. 3(b) with nearly equal profile as shown in Fig. 3(a). Compared to the comb spectrum in Fig. 3(a), one mode is suppressed by approximately 30 dB in every two modes. The mode spacing thus becomes twice that of Fig. 3(a), suggesting the presence of second harmonic mode locking. The inset also shows the significant suppression of fundamental tone. The mode spacing is now 0.28 nm, corresponding to a repetition rate of 35 GHz. Similarly, for I_{SOA} = 199.7 mA, V_{SA} = 1.05 V, Fig. 3(c) shows a fourth harmonic mode-locking spectrum with a 36-dB suppression ratio and 0.56-nm mode spacing, equivalent to 70 GHz. However, 70 GHz is above the 50-GHz spectrum analyzer bandwidth. Fig. 3(d) shows the superimposed optical spectra under PML conditions with selected DBR injection currents. By tuning the injection current I_{DBR}, the DBR stopband moves towards shorter wavelengths, subsequently blue-shifting the PML spectra. A controllable shift of ∼3 nm is observed for I_{DBR} = 0 - 50 mA. These confirm the switchability of harmonic order and wavelength by adjusting the DC operation conditions.

4. Conclusion

We have proposed a colliding-pulse PML comb laser developed with the generic foundry approach in an open-access MPW fabrication run. We demonstrate the switching between the fundamental, second, and fourth order of harmonic mode locking and a wavelength tuning range of 3 nm using DC control.

Acknowledgement

This project has received funding from the EU H2020 Marie Skłodowska-Curie grant agreement No. 101032236. We thank G. Binet, O. Abdeen, and M. Baier from Fraunhofer HHI for providing fabrication and suggestions.

References

1. Marin-Palomo, Pablo, et al. “Performance of chip-scale optical frequency comb generators in coherent WDM communications.” Optics express 28.9 (2020): 12897-12910.
2. Koenig, Swen, et al. “Wireless sub-THz communication system with high data rate.” Nature photonics 7.12 (2013): 977-981.
3. Zhou, Zichuan, et al. “Simultaneous Clock and RF Carrier Distribution for Beyond 5G Networks Using Optical Frequency Comb.” ECOC 2022
4. Hermans, Artur, Kasper Van Gasse, and Bart Kuyken. “On-chip optical comb sources.” APL Photonics 7.10 (2022): 100901.
5. Arahira, Shin, Yasuhiro Matsui, and Yoh Ogawa. “Mode-locking at very high repetition rates more than terahertz in passively mode-locked distributed-Bragg-reflector laser diodes.” IEEE journal of quantum electronics 32.7 (1996): 1211-1224.
6. Smit, Meint, Kevin Williams, and Jos Van Der Tol. “Past, present, and future of InP-based photonic integration.” APL Photonics 4.5 (2019): 050901.
7. Van Gasse, Kasper, et al. “Recent advances in the photonic integration of mode-locked laser diodes.” IEEE Photonics Technology Letters 31.23 (2019): 1870-1873.
8. Liu, Songtao, et al. “AWG-Based Monolithic 4 × 12 GHz Multichannel Harmonically Mode-Locked Laser.” IEEE Photonics Technology Letters 28.3 (2015): 241-244.
9. Nielsen, Lars, and Martijn JR Heck. “Fully integrated 45-GHz harmonically mode-locked ring laser with an intra-cavity Mach–Zehnder filter.” Optics Letters 46.4 (2021): 880-883.
10. Latkowski, Sylwester, et al. “Monolithically integrated 2.5 GHz extended cavity mode-locked ring laser with intracavity phase modulators.” Optics Letters 40.1 (2015): 77-80.
11. Moskalenko, V., K. A. Williams, and E. A. J. M. Bente. “Pulse narrowing and RF linewidth reduction of integrated passively mode-locked laser in anticolliding design by means of spectral tuning.” IEEE Photonics Journal 8.4 (2016): 1-10.
12. Soares, Francisco M., et al. “InP-based foundry PICs for optical interconnects.” Applied Sciences 9.8 (2019): 1588.